

Neurodegeneration Induced by Clustering of Sialylated Glycosylphosphatidylinositols of Prion Proteins*

Received for publication, June 24, 2011, and in revised form, January 18, 2012 Published, JBC Papers in Press, January 20, 2012, DOI 10.1074/jbc.M111.275743

Clive Bate^{‡1} and Alun Williams[§]

From the [‡]Department of Pathology and Infectious Diseases, Royal Veterinary College, Hawkshead Lane, North Mymms, Hatfield, Hertfordshire AL9 7TA and the [§]Department of Veterinary Medicine, University of Cambridge, Madingley Road, Cambridge CB3 0ES, United Kingdom

The transmissible spongiform encephalopathies, more commonly known as the prion diseases, are associated with the production and aggregation of disease-related isoforms of the prion protein (PrP^{Sc}). The mechanisms by which PrP^{Sc} accumulation causes neurodegeneration in these diseases are poorly understood. In cultured neurons, the addition of PrP^{Sc} alters cell membranes, increasing cholesterol, activating cytoplasmic phospholipase A₂ (cPLA₂), and triggering synapse damage. These effects of PrP^{Sc} are dependent upon its glycosylphosphatidylinositol (GPI) anchor, suggesting that it is the increased density of GPIs that occurs following the aggregation of PrP^{Sc} molecules that triggers neurodegeneration. This hypothesis was supported by observations that cross-linkage of the normal cellular prion protein (PrP^C) also increased membrane cholesterol, activated cPLA₂, and triggered synapse damage. These effects were not seen after cross-linkage of Thy-1, another GPI-anchored protein, and were dependent on the GPI anchor attached to PrP^C containing two acyl chains and sialic acid. We propose that the aggregation of PrP^{Sc}, or the cross-linkage of PrP^C, causes the clustering of sialic acid-containing GPI anchors at high densities, resulting in altered membrane composition, the pathological activation of cPLA₂, and synapse damage.

The cellular prion protein (PrP^C)² is a glycosylphosphatidylinositol (GPI)-anchored glycoprotein (1), which is abundantly expressed on neurons. Although the precise role of PrP^C in neurons is unclear, observations that it is concentrated at synapses (2, 3) led to suggestions that it regulates neurotransmission (4). The conversion of PrP^C into an alternatively folded, disease-associated conformation (PrP^{Sc}) is the key event leading to the prion diseases (5). This change in structure is accompanied by changes in the biochemical properties, including a capacity to self-aggregate, resulting in PrP^{Sc} oligomers (6). The accumulation of PrP^{Sc} oligomers leads to the loss of synapses and consequently the clinical signs of infection. However, the molecular mechanisms by which PrP^{Sc} causes synapse degeneration remain poorly understood.

Although GPIs were originally regarded as simple anchors that tethered proteins to cell membranes, it is now recognized that GPIs are involved in protein sorting and cell signaling (7). An increasing number of GPI-anchored proteins including CD59 (8), Thy-1 (9), CD14 (10), and Fc- ϵ -R1 (11) are associated with cell responses and the activation of multiple cell-signaling pathways. The diversity of responses that follow the engagement of GPI-anchored receptors may reflect diversity in the composition and structure of GPI anchors. Although the core of GPI anchors is conserved (7, 12), they have variable glycan side chains and lipid moieties, and there is increasing interest in the physiological significance of such variations. Cell activation commonly occurs following cross-linkage of GPI-anchored proteins by antibodies (10, 14), suggestive of a density-dependent effect.

Although several studies have examined the role of the GPI in PrP^{Sc} formation (15, 16), the first indication that GPI anchors play a role in the pathogenesis of prion disease was when transgenic mice producing anchorless PrP^C that were infected with scrapie were reported to produce large amounts of PrP^{Sc} without suffering clinical disease (17). However, because these mice produce PrP^C lacking the entire GPI anchor, they failed to provide information regarding the biological effects of specific GPI anchor components. The role of GPI anchors in the biological activity of PrP^{Sc} has been difficult to determine as aggregated forms of PrP^{Sc} protect the GPIs from digestion with phosphatidylinositol-phospholipase C (PI-PLC) (18). However, a shaking technique developed to amplify small amounts of PrP^{Sc} for detection (19) allowed successful digestion of the PrP^{Sc}-GPI anchor with either PI-PLC or phospholipase A₂ (PLA₂), resulting in deacylated and monoacylated PrP proteins (20). In the current study, synapse damage induced in cultured neurons by PrP^{Sc} was reduced by digestion of PrP^{Sc} with phospholipases. Furthermore, the cross-linkage of PrP^C mimicked the effects of PrP^{Sc} on neurons and triggered synapse damage. These properties of cross-linked PrP^C were dependent on the composition of the GPI anchor and were lost after digestion with phospholipases or with neuraminidase, which removes sialic acid from the GPI anchor attached to PrP^C. We therefore propose that PrP^{Sc}-induced synapse degeneration occurs as a consequence of the clustering of specific GPI anchors at high densities in cell membranes.

EXPERIMENTAL PROCEDURES

Primary Neuronal Cultures—Cortical neurons were prepared from the brains of day 15.5 murine embryos derived from

* This work was supported by a grant from the European Commission FP6 "Neuroprion" Network of Excellence.

¹ To whom correspondence should be addressed. Tel.: 44-1707-666550; Fax: 44-1707-661464; E-mail: cbate@rvc.ac.uk

² The abbreviations used are: PrP, prion protein; PrP^C, cellular prion protein; PrP^{Sc}, disease-related isoform of PrP; GPI, glycosylphosphatidylinositol; PLA₂, phospholipase A₂; cPLA₂, cytoplasmic PLA₂; PI-PLC, phosphatidylinositol-phospholipase C; PL, phospholipase; HPTLC, high performance thin-layer chromatography; PNGase, endoglycosidase F.

Prnp wild type (+/+) or Prnp knock-out (-/-) mice. After mechanical dissociation and cell sieving, neurons were seeded at 2×10^5 cells/well in 48-well plates (precoated with poly-L-lysine) in Ham's F12 medium containing 5% fetal calf serum (FCS) for 2 h. Cultures were shaken (600 rpm for 5 min), and nonadherent cells were removed by three washes in PBS. Neurons were grown in Neurobasal medium containing B27 components for 10 days. Immunohistochemistry showed that the cells were greater than 95% neurofilament positive. To assess their effect upon synapses or the activation of cytoplasmic PLA₂ (cPLA₂), neurons were incubated with test preparations, antibodies, or Fab fragments for 24 h. In some assays, neurons were pretreated with PLA₂ inhibitors for 1 h before the addition of PrP preparations. For toxicity experiments, neurons were incubated with PrP preparations for 5 days, and cell survival was determined by the addition of 25 μ M thiazolyl blue tetrazolium for 3 h.

Cell Membrane Extracts—Treated cells were washed three times in ice-cold PBS and homogenized in an extraction buffer (10 mM Tris-HCl, pH 7.2, 100 mM NaCl, 10 mM EDTA, 0.5% Nonidet P-40, 0.5% sodium deoxycholate, and 0.2% SDS) at 10^6 cells/ml, and cell debris was removed by centrifugation ($500 \times g$ for 5 min). Mixed protease inhibitors (4-(2-aminoethyl) benzenesulfonyl fluoride, aprotinin, leupeptin, bestatin, pepstatin A, and E-46) (Sigma) and a phosphatase inhibitor mixture including PP1, PP2A, microcystin LR, cantharidin, and *p*-bromotetramisole (Sigma) were added to membrane extracts when appropriate.

PrP^{Sc} Preparations—To study the effects of PrP^{Sc} on synapses supernatants from prion-infected ScGT1 cells containing PrP^{Sc}, oligomers were centrifuged ($16,000 \times g$ for 30 min) and passed through a 0.2- μ m filter to remove large aggregates. The supernatants were concentrated so that they contained 5 ng/ml PrP and dialyzed against Neurobasal medium. Soluble PrP^{Sc} was treated with 0.2 units/ml PI-PLC (*Bacillus cereus*) or 10 units/ml bee venom PLA₂ (Sigma) as described previously (20) or with 0.2 units/ml neuraminidase (*Clostridium perfringens*) (Sigma) plus intermittent shaking for 2 h at 37 °C and heated to denature enzymes. Control preparations were incubated with heat-denatured enzymes.

Isolation of PrP^C—PrP^C was isolated by a mixture of affinity purification and reverse phase chromatography. Briefly, cell membranes from GT1 neuronal cells or from N9 glial cells were isolated following repeated homogenization in distilled water and the removal of cell debris and nuclei by centrifugation ($1000 \times g$ for 5 min). Cell membranes were further homogenized in ice-cold 1% Triton X-100 in PBS, 10 mM EDTA, and protease inhibitors for 1 h. Insoluble material was removed by centrifugation ($1000 \times g$ for 5 min), and the supernatant was incubated with mAb 4F2 and mixed. After 30 min, 10 μ l/ml protein G magnetic microbeads (Miltenyi) were added and mixed for a further 30 min. Antibody-bound complexes were collected using a magnetic bead isolation kit (Miltenyi), and beads were washed twice with cold 1% Triton X-100 and then three times with warm (37 °C) PBS containing 10 mM EDTA and protease inhibitors. Beads were subsequently incubated in PBS containing DNase and sphingomyelinase (Sigma) \pm 2 units/ml endoglycosidase F (PNGase) (Sigma), 0.2 units/ml PI-

PLC, 10 units/ml PLA₂, or 0.2 units/ml neuraminidase for 2 h at 37 °C. PrP^C/digested PrP^C was dissociated from the mAb/protein G complex using 0.1 M glycine HCl at pH 2.7 and applied to C18 columns. PrP^C was eluted under a gradient of acetonitrile in water and 0.1% trifluoroacetic acid; fractions were collected and tested in a PrP ELISA. Fractions containing PrP^C were pooled, reloaded onto a new C18 column, and eluted as before. This process was repeated, and the PrP^C-containing fractions were lyophilized and stored at -80 °C. Samples were sonicated in culture medium for bioassays. Thy-1 was also isolated from GT1 cell membranes prepared with an anti-Thy-1 mAb (Sero-tec), protein G magnetic beads, and C18 columns as described above. Fractions eluted from C18 columns were identified by dot blot and pooled and desalted, and the protein concentration was determined by a micro-BCA assay (Pierce).

Western Blot Analysis—Samples were mixed with Laemmli buffer, heated to 95 °C, and subjected to electrophoresis on 15% polyacrylamide gels. Proteins were transferred onto a Hybond-P PVDF membrane (Amersham Biosciences) by semi-dry blotting. Membranes were blocked with 10% milk powder and incubated with mAb ICSM35 (to detect PrP/cross-linked PrP^C). mAb 4H302 (Abcam) was used to detect synaptobrevin, rabbit polyclonal anti-synaptophysin (Abcam), rabbit polyclonal antibody to synapsin-1 (515200, Invitrogen), rabbit polyclonal antibodies to Na,K-ATPase α 1 subunit (Abcam), mouse mAb to β -actin, and clone AC-74 (Sigma) followed by a secondary anti-mouse or anti-rabbit IgG or anti-mouse IgG conjugated to peroxidase. Bound antibody was visualized using enhanced chemiluminescence.

Cross-linkage of Proteins—PrP^C or Thy-1 preparations were cross-linked using the homobifunctional cross-linking agent dimethyl pimelimidate (Pierce) according to the manufacturer's instructions. Dimethyl pimelimidate is a cross-linking agent that contains an amine-reactive imidoester at each end of a 9.2 Å (seven-atom) spacer arm. Cross-linked proteins and mock-treated controls were desalted using Vivaspin filters (Sartorius) and suspended in culture media. Before use, cross-linked PrP^C preparations were centrifuged at $16,000 \times g$ for 10 min and then passed through 0.2- μ m and 500-kDa filters and to remove large aggregates.

Isolation of GPI Anchors—GPIs were isolated from PrP^C or Thy-1 preparations by digestion with 100 μ g/ml proteinase K at 37 °C for 4 h. The GPIs released from PrP^C or PLA₂-digested PrP^C were extracted with water-saturated butan-1-ol and lyophilized. Samples were dissolved in ethanol and separated by high performance thin-layer chromatography (HPTLC) on Silica Gel 60 plates.

Lectin Binding Analysis of GPI Anchors—The presence of specific glycans in GPI anchors was determined using biotinylated lectins. Isolated GPI anchors were bound to nitrocellulose membranes by dot blot and blocked with 5% milk powder. Samples were incubated with biotinylated *Sambucus nigra* lectin (to detect terminal sialic acid residues bound by α -2,6 or α -2,3 to galactose) or biotinylated concanavalin A to detect mannose (Vector Laboratories). Bound lectins were visualized using ExtrAvidin peroxidase and enhanced chemiluminescence. The blotted GPI anchors were also incubated with mAb 5AB3-11 to show the presence of phosphatidylinositol.

Synaptophysin ELISA—The amount of synaptophysin in neuronal extracts was measured by ELISA as described (21). MaxiSorp immunoplates (Nunc) were coated with a mAb to synaptophysin (MAB368, Chemicon) and blocked with 10% milk powder. Samples were added for 1 h, and synaptophysin was detected using a rabbit polyclonal anti-synaptophysin (Abcam) followed by a biotinylated anti-rabbit IgG (Dako), ExtrAvidin-alkaline phosphatase, and 1 mg/ml 4-nitrophenol phosphate (Sigma). Absorbance was measured on a microplate reader at 405 nm. Samples were expressed as “units of synaptophysin” where 100 units were defined as the amount of synaptophysin in 10^6 untreated cells.

Activated cPLA₂ ELISA—The activation of cPLA₂ is accompanied by phosphorylation of the serine 505 residue, which can be measured by phospho-specific antibodies as described (21). Briefly, MaxiSorp immunoplates were coated with 0.5 μ g/ml mouse mAb anti-cPLA₂, clone CH-7 (Upstate Biotech Millipore) and blocked with 10% milk powder. Samples were incubated for 1 h, and the amount of activated cPLA₂ was detected using a rabbit polyclonal anti-phospho-cPLA₂ (Cell Signaling Technology). Bound antibodies were detected using biotinylated anti-rabbit IgG (Dako), ExtrAvidin-alkaline phosphatase, and 1 mg/ml 4-nitrophenyl phosphate. Absorbance was measured at 405 nm. Samples were expressed as “units of activated cPLA₂,” where 100 units were defined as the amount of activated cPLA₂ in 10^6 untreated neurons.

Cholesterol—The amounts of cholesterol were measured using the Amplex Red cholesterol assay kit (Invitrogen), according to the manufacturer's instructions. Briefly, cholesterol is oxidized by cholesterol oxidase to yield hydrogen peroxide, which reacts with 10-acetyl-3, 7-dihydroxyphenoxazine (Amplex Red reagent) to produce fluorescent resorufin, which is measured by excitation at 550 nm and emission detection at 590 nm. The amounts of cholesterol were calculated by reference to cholesterol standards.

Preparation of Fab Fragments—Fab fragments were prepared from mAbs with the ImmunoPure Fab preparation kit (Pierce) using immobilized papain according to the manufacturer's instructions.

Statistical Analysis—Comparison of treatment effects was carried out using Student's *t* test and analysis of variance techniques.

RESULTS

PrP^{Sc}-induced Synapse Damage Is GPI-dependent—The loss of synapses, with a corresponding reduction in synaptic proteins, is an early feature of experimental and human prion diseases (22, 23). The addition of ScGT1 cell supernatants containing PrP^{Sc} caused a dose-dependent reduction in the amount of synaptophysin in neurons, indicative of synapse damage. In contrast, supernatants from uninfected GT1 cells did not affect the synaptophysin content of neurons (data not shown). Immunodepletion with mAb ICSM35 (which binds to PrP^{Sc}) reduced the effects of ScGT1 cell supernatants upon synapses, whereas immunodepletion with mAb ICSM18 (which binds to PrP^C but not to PrP^{Sc}) had no discernable effect, indicating that the toxic entity within these supernatants was PrP^{Sc} (Fig. 1A). The role of GPI anchors in PrP^{Sc}-mediated synaptotoxicity was examined

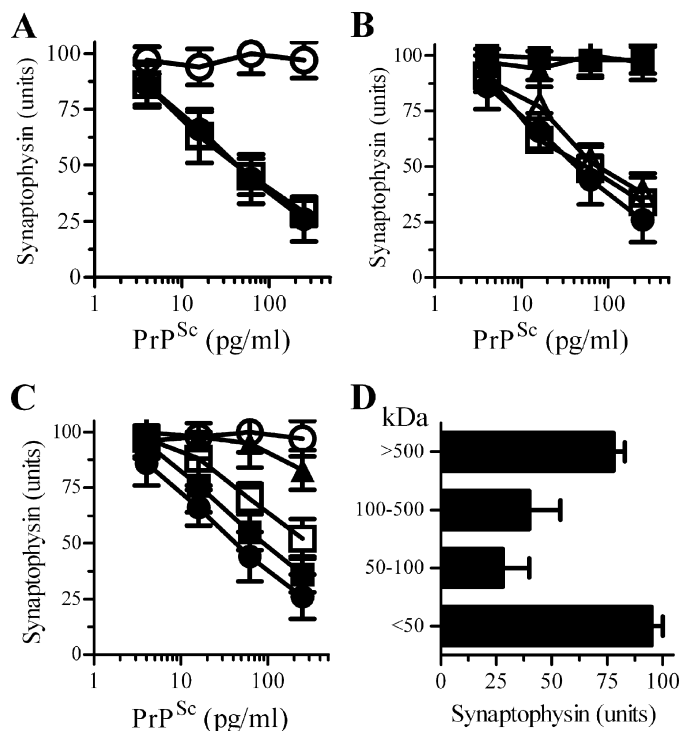


FIGURE 1. PrP^{Sc}-induced synapse damage is dependent on GPI anchors. A, the amount of synaptophysin in neurons incubated with ScGT1 cell supernatants containing PrP^{Sc} that had been mock-treated (●), immunodepleted by incubation with the PrP^{Sc}-reactive mAb ICSM35 (○), or immunodepleted by incubation with the PrP^C-reactive mAb ICSM18 (□). Values shown are the mean units of synaptophysin \pm S.D. from triplicate experiments performed four times, $n = 12$. B, the amount of synaptophysin in neurons incubated with ScGT1 cell supernatants containing PrP^{Sc} that had been incubated with control medium (●), PI-PLC (■), heat-denatured PI-PLC (□), PLA₂ (▲), or heat-denatured PLA₂ (△). Values shown are the mean units of synaptophysin \pm S.D. from triplicate experiments performed four times, $n = 12$. C, the amount of synaptophysin in neurons incubated with ScGT1 cell supernatants containing PrP^{Sc} (●), ScGT1 cell supernatants that had been passed through a 50-kDa filter (○), a 100-kDa filter (□), or a 500-kDa filter (■), or ScGT1 supernatants greater than 500 kDa (▲). Values shown are the mean units of synaptophysin \pm S.D. from triplicate experiments performed three times, $n = 9$. D, the amount of synaptophysin in neurons incubated with ScGT1 cell supernatants containing PrP^{Sc} that had been separated into different sized oligomers by sequential passage through 50-, 100-, and 500-kDa filters. Values shown are the mean units of synaptophysin \pm S.D. from triplicate experiments performed four times, $n = 12$.

by digestion of ScGT1 cell supernatants with PI-PLC or PLA₂. The addition of mock-treated PrP^{Sc} reduced the synaptophysin content of neurons, whereas PI-PLC-digested PrP^{Sc} (deacylated PrP^{Sc}) and PLA₂-digested PrP^{Sc} (monoacylated PrP^{Sc}) had little effect (Fig. 1B), indicating that the GPI anchors play a major role in the synaptotoxicity of PrP^{Sc}. PrP^{Sc} preparations that had been incubated with heated-denatured PI-PLC or PLA₂ (100 °C for 5 min) had similar effects as mock-treated PrP^{Sc} preparations. To determine whether synapse damage was associated with specific sized oligomers, ScGT1 supernatants were passed through different pore-sized filters. Most of the toxic entities in ScGT1 cell supernatants passed through a 500-kDa filter, indicating that small PrP^{Sc} oligomers were responsible for synapse damage rather than larger aggregates (Fig. 1, C and D). More specifically, synapse damage was seen in neurons incubated with supernatants that passed through a 100-kDa filter but not with supernatants that passed through a 50-kDa filter.

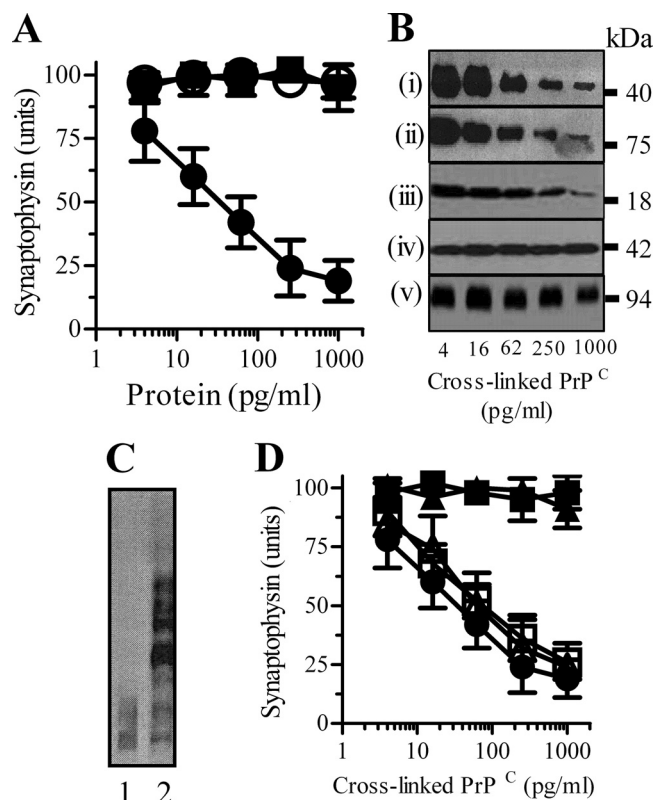


FIGURE 2. Cross-linked PrP^C-induced synapse damage is dependent on GPI anchors. **A**, the amount of synaptophysin in neurons incubated with cross-linked PrP^C (●), mock-treated PrP^C (○), or cross-linked Thy-1 (■). Values shown are the mean units of synaptophysin \pm S.D. from triplicate experiments performed four times, $n = 12$. **B**, immunoblots showing the amount of synaptophysin (i), synapsin-1 (ii), synaptobrevin (iii), β -actin (iv), or Na,K-ATPase α 1 subunit (v) in extracts from neurons incubated for 24 h with cross-linked PrP^C as shown. **C**, immunoblot showing preparations of mock-treated PrP^C (lane 1) or cross-linked PrP^C (lane 2). **D**, the amount of synaptophysin in neurons incubated with cross-linked PrP^C that had been pretreated with control medium (●), PI-PLC (■), heat-denatured PI-PLC (□), PLA₂ (▲), or heat-denatured PLA₂ (△). Values shown are the mean units of synaptophysin \pm S.D. from triplicate experiments performed four times, $n = 12$.

Cross-linked PrP^C Damages Synapses—The self-aggregation of PrP^{Sc} molecules results in the clustering of GPI anchors at high densities within cell membranes. Because cell activation by some GPI-anchored proteins is associated with the clustering of proteins (24, 25), we hypothesized that the synapse damage induced by PrP^{Sc} was mediated by the increased density of GPI anchors that occurs following the aggregation of PrP^{Sc}. To test this hypothesis, we sought to mimic the effects of PrP^{Sc} by cross-linking PrP^C molecules. Cortical neurons were incubated with preparations containing cross-linked PrP^C or mock-treated PrP^C. Cross-linked PrP^C caused a dose-dependent reduction in the synaptophysin content of neurons, indicative of synapse damage that was not seen with mock-treated PrP^C (Fig. 2A). The synaptophysin content of neurons was reduced by greater than 80% by 1 ng/ml cross-linked PrP^C, which did not affect neuronal survival as measured by thiazolyl blue tetrazolium (98% neuronal survival \pm 6 as compared with mock-treated cells 100% \pm 6, $n = 9$, $p = 0.53$). The synaptophysin content of neurons was not affected by incubation with preparations containing cross-linked Thy-1, a protein that also contains a GPI anchor. Immunoblots showed that incubation with cross-linked PrP^C reduced the amounts of the synaptic proteins

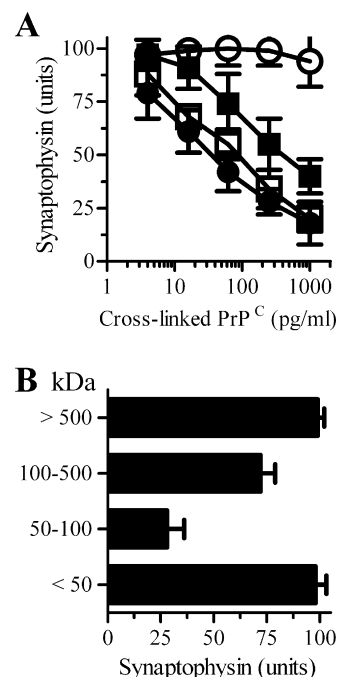


FIGURE 3. Synapse damage is caused by low-n oligomers of cross-linked PrP^C. **A**, the amount of synaptophysin in neurons incubated with cross-linked PrP^C (●) or cross-linked PrP^C preparations that had been passed through a 50-kDa filter (○), a 100-kDa filter (■), or a 500-kDa filter (□). Values shown are the mean units of synaptophysin \pm S.D. from triplicate experiments performed four times, $n = 12$. **B**, the amount of synaptophysin in neurons incubated with 1 ng/ml cross-linked PrP^C that had been separated into different sizes as shown by sequential passage through 50-, 100-, and 500-kDa filters. Values shown are the mean units of synaptophysin \pm S.D. from triplicate experiments performed four times, $n = 12$.

synaptophysin, synapsin-1, and synaptobrevin in neurons without affecting the amount of β -actin or the plasma membrane marker Na,K-ATPase α 1 subunit (Fig. 2B). An immunoblot showed that cross-linked PrP^C preparations contained mostly low-n PrP^C oligomers and unlinked PrP^C (Fig. 2C). Next, PrP^C was digested with PI-PLC or PLA₂ and isolated on C18 columns. They were subsequently cross-linked and incubated with neurons. Although the addition of cross-linked PrP^C reduced the synaptophysin content of neurons, cross-linked deacylated PrP^C or cross-linked monoacylated PrP^C had no discernible effect (Fig. 2D). Cross-linked PrP^C that had been incubated with heat-denatured PI-PLC or PLA₂ had similar toxic effects to cross-linked PrP^C. Next, cross-linked PrP^C preparations were passed through filters with different sized pores to estimate the size of the toxic oligomers. None of the toxic entities within cross-linked PrP^C preparations passed through a 50-kDa filter (Fig. 3A). Most of the toxic cross-linked PrP^C preparations passed through a 100-kDa filter, indicating that they were mainly low-n oligomers (Fig. 3B).

Contaminating Proteins Reduce Toxicity of Cross-linked PrP^C Preparations—Although the preparations used were highly enriched for PrP^C, we recognize that they were not pure. To determine whether the presence of contaminating proteins affected their activity, PrP^C preparations were mixed with equimolar concentrations of bovine serum albumin (BSA), Thy-1, or deacylated PrP^C and cross-linked to produce hetero-oligomers. We report that hetero-oligomers containing 1 ng/ml

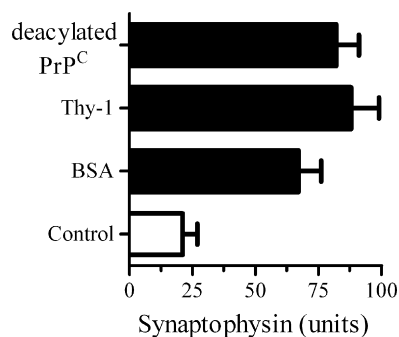


FIGURE 4. **Contaminating proteins reduce toxicity of cross-linked PrP^C.** 1 ng/ml PrP^C was mixed with control medium (□) or with equimolar concentrations of BSA, Thy-1, or deacylated PrP^C (■) as shown. The mixtures were cross-linked and incubated with neurons for 24 h when the amount of synaptophysin remaining in neurons was measured. Values shown are the mean units of synaptophysin \pm S.D. from triplicate experiments performed five times, $n = 15$.

PrP^C and BSA, Thy-1, or deacylated PrP^C caused less synapse damage than homo-oligomers of PrP^C (Fig. 4).

Removal of Sialic Acids from GPI Anchor Reduces Synaptotoxicity of Cross-linked PrP^C—Because the glycan composition of GPIs attached to some proteins is cell line-specific (26), the effects of PrP^C derived from a glial cell line were examined. Preparations containing cross-linked PrP^C derived from glial cells did not cause synapse damage (Fig. 5A), suggesting that synapse damage occurs in response to the clustering of GPI anchors with a specific glycan composition. HPTLC analysis showed that the GPIs isolated from PrP^C derived from neuron and glial cells were different (Fig. 5B). The GPI attached to PrP^C has been reported to contain sialic acid, a rare modification of mammalian GPI anchors (1). To confirm the presence of sialic acid, GPI anchors were probed with biotinylated lectins. *S. nigra* lectin (which reacts with terminal sialic acid bound by either α -2,6 or α -2,3 to galactose) bound to GPI anchors isolated from neuron-derived PrP^C, but not to GPI anchors isolated from glia-derived PrP^C. The binding of the mannose-binding lectin concanavalin A or the phosphatidylinositol-specific mAb 5AB3-11 demonstrated that similar amounts of GPI anchors were loaded on each blot (Fig. 5C).

To examine the effects of the sialic acid on the function of GPI anchors, PrP^C was digested with neuraminidase, resulting in desialylated PrP^C. HPTLC analysis showed that neuraminidase digestion altered the GPI anchor attached to neuron-derived PrP^C (Fig. 6A). Neuraminidase digestion of neuron-derived PrP^C resulted in a GPI anchor that bound readily to concanavalin A and the phosphatidylinositol-selective mAb 5AB3-11, but did not bind to *S. nigra* lectin (Fig. 6B). Because neuraminidase can affect sialic acids expressed on *N*-linked glycans as well as those on the GPI anchor, the *N*-linked glycans attached to PrP^C were removed by PNGase digestion (27). There was no significant difference in the synaptophysin content of neurons incubated with cross-linked PrP^C and those incubated with cross-linked PNGase-digested PrP^C, indicating that the *N*-linked side chains did not play a significant role in synapse damage. PNGase-digested PrP^C was then digested with neuraminidase and cross-linked. Preparations containing cross-linked PrP^C that had been digested with PNGase and neuraminidase did not cause synapse damage, indicating that

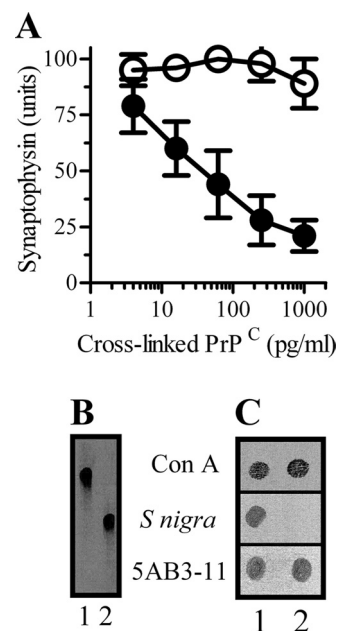


FIGURE 5. **Cross-linked, glia-derived PrP^C does not damage synapses.** A, the amount of synaptophysin in neurons incubated with cross-linked, neuron-derived PrP^C (●) or cross-linked, glia-derived PrP^C (○). Values shown are the mean units of synaptophysin \pm S.D. from triplicate experiments performed three times, $n = 9$. B, HPTLC showing GPI anchors isolated from neuron-derived PrP^C (lane 1) or glia-derived PrP^C (lane 2) and separated in a solution of methanol/chloroform/water on silica 60 plates. C, dot blots showing the binding of biotinylated concanavalin A (Con A), biotinylated *S. nigra*, and mAb 5AB3-11 to GPI anchors isolated from neuron-derived PrP^C (lane 1) or glia-derived PrP^C (lane 2).

the sialic acid expressed upon the GPI anchor was essential for synapse damage (Fig. 6C). Pretreatment with heat-denatured neuraminidase did not affect cross-linked PrP^C-induced synapse damage.

Cross-linked PrP^C Increases Membrane Cholesterol in Synapses—The level of cholesterol in cell membranes is an important factor in the progression of prion diseases (28–30). PrP^{Sc} increases the amount of cholesterol in cell membranes, and because cholesterol is essential for the maintenance of synapses (31), the effects of PrP^{Sc}, PrP^C, and cross-linked PrP^C upon the amount of cholesterol in synaptosomes was examined. Neurons were treated for 1 h, and synaptosomes were isolated. The amount of cholesterol in treated synaptosomes was significantly increased in comparison with control neurons following incubation with 1 ng of PrP^{Sc} or with 1 ng of cross-linked PrP^C, but not after incubation with 1 ng of mock-treated PrP^C (Table 1). The addition of cross-linked deacylated PrP^C or cross-linked monoacylated PrP^C did not alter the amount of cholesterol in neuronal membranes, nor did the addition of deacylated PrP^{Sc} or monoacylated PrP^{Sc}.

PrP^{Sc} and Cross-linked PrP^C Activate cPLA₂—The activation of cPLA₂ is a key event in neurodegenerative diseases including prion and Alzheimer diseases (32–34). More specifically, the activation of cPLA₂ at synapses causes synapse damage in cultured neurons (21). In this study, the addition of PrP^{Sc} increased the amount of activated cPLA₂ in synaptosomes, whereas the addition of deacylated PrP^{Sc} or monoacylated PrP^{Sc} had little effect (Fig. 7A). Similarly, the addition of cross-linked, neuron-derived PrP^C increased the amount of activated

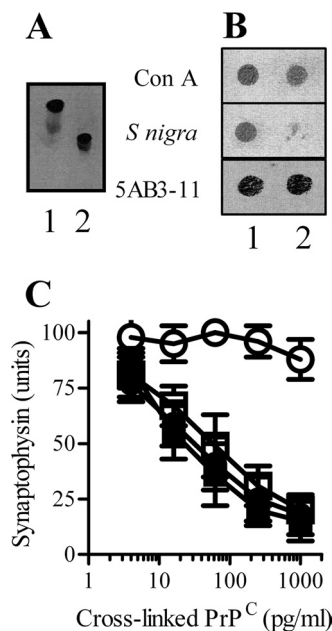


FIGURE 6. Neuraminidase digestion reduced neurotoxicity of cross-linked PrP^C. A, HPTLC showing the migration of GPI anchors isolated from PrP^C (lane 1) or neuraminidase-digested PrP^C (lane 2) separated in a solution of methanol/chloroform/water on silica 60 plates. B, dot blots showing the binding of biotinylated concanavalin A (Con A), biotinylated *S. nigra*, and mAb 5AB3-11 to GPI anchors isolated from PrP^C (lane 1) or neuraminidase-digested PrP^C (lane 2). C, the synaptophysin content of neurons incubated with cross-linked PrP^C (●) or cross-linked PrP^C that had been digested with PNGase and neuraminidase (○), PNGase (□), or PNGase and heat-denatured neuraminidase (■). Values shown are the mean units of synaptophysin ± S.D. from triplicate experiments performed four times, *n* = 12.

TABLE 1

Structure of GPI anchor affects membrane cholesterol

The amount of cholesterol in synaptosomes from neurons incubated for 1 h with 1 ng/ml cross-linked PrP^C or 1 ng/ml PrP^{Sc} that had been digested with enzymes as shown. The amount of cholesterol in synaptosomes derived from untreated neurons was 92 ng/10⁶ cells ± 9. Values shown are the mean amount of cholesterol in synaptosomes (ng/10⁶ cells) ± S.D. from triplicate experiments performed four times, *n* = 12.

Treatment	Cholesterol (ng/10 ⁶ cells)	
	Cross-linked PrP ^C	PrP ^{Sc}
None	125 ± 9 ^a	129 ± 17 ^a
PI-PLC	96 ± 13	89 ± 9
Denatured PI-PLC	124 ± 15 ^a	123 ± 12 ^a
PLA ₂	99 ± 10	93 ± 8
Denatured PLA ₂	130 ± 11 ^a	133 ± 14 ^a
PNGase	128 ± 18 ^a	126 ± 10 ^a
Neuraminidase	123 ± 14 ^a	128 ± 9 ^a

^a Amount of cholesterol significantly higher than that of synaptosomes from untreated neurons (*p* < 0.05).

cPLA₂ in synaptosomes, whereas mock-treated neuron-derived PrP^C or cross-linked, glia-derived PrP^C had little effect (Fig. 7B). Next, the modifications of GPI anchors that reduced synapse damage in response to cross-linked, neuron-derived PrP^C were tested for their effects on the activation of cPLA₂ in synaptosomes. We report that cross-linked deacylated PrP^C, cross-linked monoacylated PrP^C, or cross-linked desialylated PrP^C had a lesser effect upon activation of synaptic cPLA₂ than cross-linked PrP^C (Fig. 7C). To confirm a causal role of activated cPLA₂ in the synapse damage induced by cross-linked PrP^C, neurons were pretreated with cPLA₂ inhibitors. Pretreatment with 1 μM archidonyl trifluoromethyl ketone or 2 μM methyl archedonyl fluorophosphate protected neurons

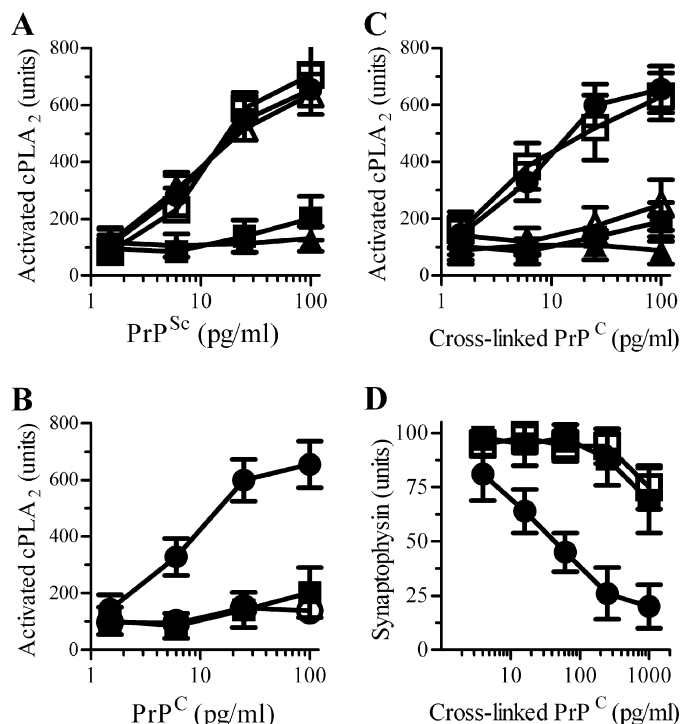


FIGURE 7. PrP-induced activation of cPLA₂ is dependent on GPI anchors. A, the amount of activated cPLA₂ in synaptosomes incubated with PrP^{Sc} that had been pretreated with control medium (●), PI-PLC (■), heat-denatured PI-PLC (□), PLA₂ (▲), or heat-denatured PLA₂ (△). Values shown are the mean units of activated cPLA₂ ± S.D. from triplicate experiments performed three times, *n* = 9. B, the amount of activated cPLA₂ in neurons incubated with neuron-derived PrP^C (○), cross-linked neuron-derived PrP^C (●), or cross-linked glia-derived PrP^C (■). Values shown are the mean units of activated cPLA₂ ± S.D. from triplicate experiments performed three times, *n* = 9. C, the amount of activated cPLA₂ in neurons incubated with cross-linked PrP^C that had been pretreated with control medium (●), PI-PLC (■), heat-denatured PI-PLC (□), PLA₂ (▲), or neuraminidase (△). Values shown are the mean units of activated cPLA₂ ± S.D. from triplicate experiments performed three times, *n* = 9. D, the amount of synaptophysin in neurons pretreated with control medium (●), 1 μM archidonyl trifluoromethyl ketone (□), or 2 μM methyl archedonyl fluorophosphate (■) and incubated with cross-linked PrP^C. Values shown are the mean units of synaptophysin ± S.D. from triplicate experiments performed four times, *n* = 12.

against the cross-linked PrP^C-induced synapse damage (Fig. 7D).

Cross-linkage of PrP^C by mAbs Induces Cell Signaling and Synapse Damage—Some of the effects of PrP^{Sc} can be mimicked by the cross-linkage of PrP^C with mAbs, which leads to cell signaling in T cells (35) and neurodegeneration (36). Here we show that the addition of mAb 4F2 caused synapse damage to cultured Prnp^{+/+} neurons, whereas the monovalent Fab fragments prepared from this mAb had little effect (Fig. 8A). Similarly, mAb 4F2 caused a dose-dependent increase in the amount of activated cPLA₂ in synaptosomes, whereas Fab fragments had no effect (Fig. 8B).

To examine further the role of the GPI anchor in the cell signaling and neurodegeneration induced by PrP^C-reactive mAbs, 10⁶ Prnp^{-/-} neurons were pretreated with different concentrations of PrP^C, monoacylated PrP^C, or desialylated PrP^C for 2 h, and the amount of cell-associated PrP^C was determined by ELISA. Greater amounts of monoacylated PrP^C were incorporated into neurons than either PrP^C or desialylated PrP^C (Fig. 9A). Next, 10⁶ Prnp^{-/-} neurons were pretreated

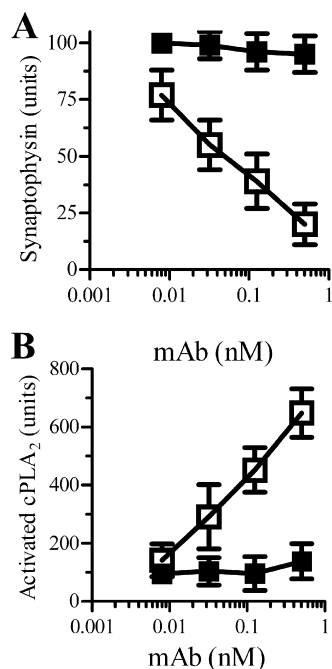


FIGURE 8. mAb-mediated cross-linkage of PrP^{Sc} causes synapse damage. A, the amount of synaptophysin in Prnp^{+/+} neurons that had been incubated with mAb 4F2 (□) or Fab fragments isolated from 4F2 (■) for 24 h. Values shown are the mean units of synaptophysin ± S.D. from triplicate experiments performed three times, *n* = 9. B, the amount of activated cPLA₂ in synaptosomes derived from Prnp^{+/+} neurons that had been incubated with mAb 4F2 (□) or Fab fragments isolated from 4F2 (■) for 24 h. Values shown are the mean units of activated cPLA₂ ± S.D. from triplicate experiments performed three times, *n* = 9.

with 10 ng of PrP^C, monoacylated PrP^C, PNGase-digested PrP^C, or desialylated PrP^C for 2 h and then incubated with serial dilutions of mAb 4F2. The addition of mAb 4F2 did not affect untreated neurons Prnp^{-/-} neurons but caused a dose-dependent reduction in the synaptophysin content of Prnp^{-/-} neurons pretreated with either PrP^C or PNGase-digested PrP^C. Notably, mAb 4F2 did not cause synapse damage in neurons pretreated with monoacylated PrP^C or desialylated PrP^C (Fig. 9B). Similarly, mAb 4F2 did not alter the amount of activated cPLA₂ in synaptosomes from untreated Prnp^{-/-} neurons but caused a dose-dependent increase in the amount of activated cPLA₂ in synaptosomes pretreated with PrP^C or with PNGase-digested PrP^C. mAb 4F2 did not activate cPLA₂ in Prnp^{-/-} synaptosomes pretreated with monoacylated PrP^C or desialylated PrP^C (Fig. 9C).

DISCUSSION

The molecular mechanisms by which PrP^{Sc} leads to neurodegeneration in prion diseases are poorly understood. Although the differences in the protein structure between PrP^C and PrP^{Sc} have been extensively studied, the effects of the clustered GPI anchors that result from the aggregation of PrP^{Sc} have been largely overlooked. In this study, we show that the clustering of sialic acid-containing GPIs attached to PrP proteins altered the composition of cell membranes, leading to increased activation of cPLA₂ and resulting in synapse damage.

The digestion of PrP^{Sc} with PI-PLC or PLA₂ reduced its effects on synapses, indicating that the synapse damage induced by PrP^{Sc} was GPI-dependent. The hypothesis that the

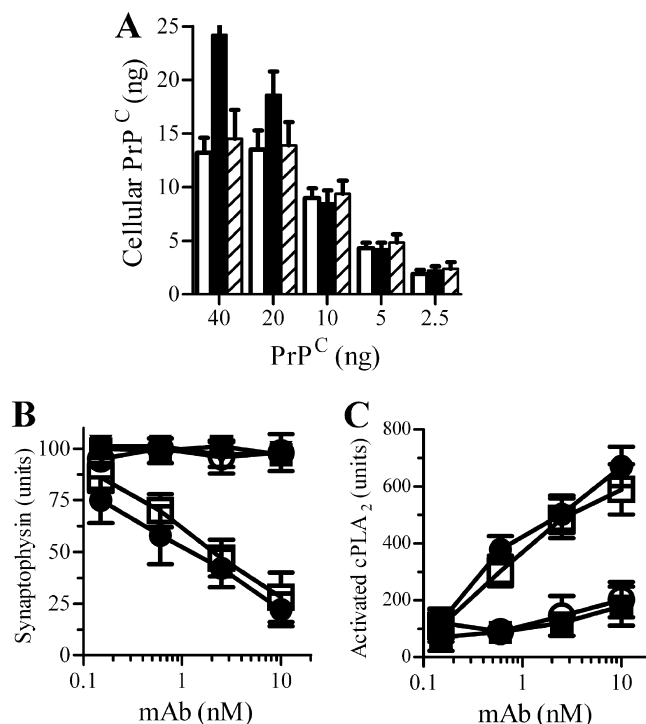


FIGURE 9. Sialic acids on GPI anchor are required for mAb-induced synapse damage. A, the amount of PrP^C in Prnp^{-/-} neurons that had been incubated with different amounts of PrP^C (□), monoacylated PrP^C (■), or desialylated PrP^C (striped bars) for 2 h. Values shown are the mean amount of PrP^C (ng/10⁶ neurons) ± S.D. from triplicate experiments performed three times, *n* = 9. B, the amount of synaptophysin in Prnp^{-/-} neurons that had been pretreated with 10 ng of PrP^C (□), 10 ng of PNGase-digested PrP^C (●), 10 ng of monoacylated PrP^C (■), or 10 ng of desialylated PrP^C (○) and incubated with mAb 4F2 for 24 h. Values shown are the mean units of synaptophysin ± S.D. from triplicate experiments performed four times, *n* = 12. C, the amount of activated cPLA₂ in synaptosomes in Prnp^{-/-} neurons that had been pretreated with 10 ng of PrP^C (□), 10 ng of PNGase-digested PrP^C (●), 10 ng of monoacylated PrP^C (■), or 10 ng of desialylated PrP^C (○) and incubated with mAb 4F2 for 24 h. Values shown are the mean units of activated cPLA₂ ± S.D. from triplicate experiments performed four times, *n* = 12.

neurotoxicity of PrP^{Sc} was due to the clustering of their GPI anchors was supported by further observations that the effects of PrP^{Sc} on synapses were replicated by cross-linked PrP^C. Mock-treated PrP^C did not have the same effects, indicating that it is the aggregation of PrP^C, and hence the density of GPI anchors, that is the important factor in generating synapse damage. Such observations are consistent with *in vivo* studies where naturally aggregated PrP^C is associated with synaptic abnormalities (37). The concentrations of cross-linked PrP^C and PrP^{Sc} required for these activities were remarkably similar, results consistent with observations that the conversion from PrP^C to PrP^{Sc} does not entail changes to the GPI anchor (1). Filtration of ScGT1 supernatants or cross-linked PrP^C preparations showed that the toxic entities were predominantly low-n oligomers of less than 100 kDa. The gradual accumulation of PrP^{Sc} in prion diseases is thought to cause synapse damage at early stages of infection where the concentrations of PrP^{Sc} in the brain are relatively low (23). In this study, the concentrations of PrP^{Sc} or cross-linked PrP^C required to cause synapse damage *in vitro* did not cause a significant loss of neuronal viability.

The synaptophysin content of neurons was not affected by incubation with cross-linked Thy-1. The GPI anchors attached

Synapse Damage in Prion Diseases

to Thy-1 and PrP^C have different glycans (1, 38), suggesting that neurodegeneration resulted from the aggregation of GPI anchors with a specific composition. The GPI anchor attached to PrP^C is unusual in that it contains sialic acid (1). This sialic acid moiety was a key element in the toxicity of the GPI anchors as the removal of sialic acid resulted in PrP^C that, when cross-linked, did not cause synapse damage. The exact role of sialic acid is unclear. It may mediate interactions between PrP^C and sialic acid-binding proteins, or it may compete with other sialic acid-containing compounds, such as the sphingolipids for sialic acid-binding proteins. PrP^C extracted from hamster brains contained PrP^C molecules attached to different GPIs, some of which did not contain sialic acid (1). The composition of the GPI anchor attached to specific proteins may be cell type-specific (26), and we found that the GPI anchor attached to PrP^C derived from glial cells (and from some neuronal cell lines)³ does not contain sialic acid. The oligomers formed by cross-linkage of glia-derived PrP^C did not cause significant synapse damage, an observation that suggests that PrP^{Sc} oligomers made by these cells would also show little toxicity. This observation may help to explain the lack of neuronal damage in the presence of high concentrations of PrP^{Sc} in different models of prion infection.

Disturbances in neuronal cholesterol metabolism are a feature of many neurodegenerative diseases (39–41). Both PrP^C and PrP^{Sc} are found within cholesterol-dense lipid rafts (42, 43), and the addition of either PrP^{Sc} or cross-linked PrP^C increased the amount of cholesterol in synaptosomes. However, this effect was not specific to cross-linked PrP^C; it was also observed following the addition of cross-linked preparations of Thy-1 or desialylated PrP^C, suggesting that the increase in cholesterol alone is not sufficient to trigger synapse damage. The effects of PrP^{Sc} or cross-linked PrP^C on membrane cholesterol were lost after digestion with PI-PLC or PLA₂, an observation that is consistent with the idea that most GPI anchors contain saturated fatty acids, which are responsible for the increased solubility of cholesterol (44). Although insufficient in itself to initiate pathology, changes in cholesterol levels may affect synapse function as the increase in cholesterol alters membrane fluidity and cholesterol is required for synapse formation (31).

Because the lipids that surround raft-associated proteins are dependent upon multiple glycan-lipid, protein-lipid, and lipid-lipid interactions (45), the specific molecular structure of the PrP^C-GPI anchor may have a direct effect on the size, composition, and function of lipid rafts. This hypothesis is supported by the observations that PrP^C and Thy-1 have different GPI anchors (1, 38) and that the domain surrounding PrP^C differs from that surrounding Thy-1 (46). Thus, any modification of the GPI anchor attached to PrP^C would be expected to alter the composition of the surrounding lipids. We propose that the membranes surrounding PrP^C differed from those surrounding either monoacylated PrP^C or desialylated PrP^C as shown in Fig. 10A.

These results suggest that it is the self-aggregation of PrP^{Sc}, or cross-linkage of PrP^C, that results in high densities of the

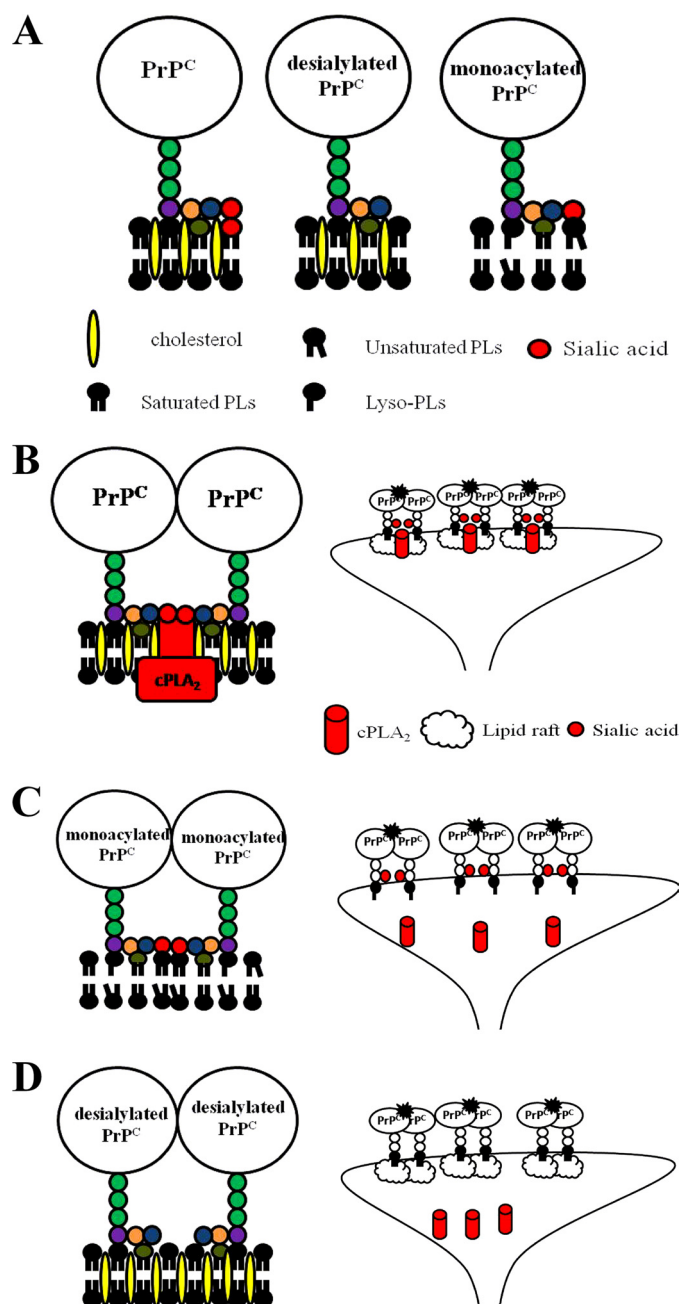


FIGURE 10. Sialic acids on GPI anchor are required for activation of cPLA₂ by cross-linked PrP^C. A, graphic showing a model of PrP^C, monoacylated PrP^C, desialylated PrP^C, and their proposed effects on the surrounding membrane domains including cholesterol, lyso-PLs, saturated PLs, and unsaturated PLs. B, cross-linkage of PrP^C with a conventional GPI anchor that contains sialic acid stabilizes and activates cPLA₂ within cholesterol-dense lipid rafts. C, cross-linkage of monoacylated PrP^C does not sequester cholesterol that is required for the formation of lipid rafts and the activation of cPLA₂. D, cross-linkage of desialylated PrP^C provides the lipid raft environment, but the lack of sialic acid moieties fails to stabilize cPLA₂ within the membrane.

PrP-attached GPI anchors that lead to synapse damage and neuronal death. The composition and function of platforms formed following the coalescence of lipid rafts are dependent upon an induced-fit model (47). Lipid rafts can coalesce to form membrane platforms in which signaling complexes assemble (48). Such platforms are frequently termed signalosomes when their constituent parts combine to activate cells. For example, in T and B cell receptor signaling, the coalescence of membrane

³ C. Bate and A. Williams, unpublished data.

proteins in the outer leaflet of lipid rafts affects the cytoplasmic leaflet and its association with signaling molecules (11, 49, 50) and leads to cell activation (51). PrP^C is associated with several signaling molecules including tyrosine kinases (52), protein kinase A (53), and cPLA₂ (21). Here we show that the PrP^{Sc}-induced or cross-linked PrP^C-induced activation of cPLA₂, which is recognized as a key event in some neurodegenerative diseases (13), was dependent upon sialic acid and two acyl chains attached to the GPI anchor. Thus, we speculate that the platform formed by cross-linkage of PrP^C contains cholesterol and a high density of sialic acids that are required to activate cPLA₂ (Fig. 10B). In contrast, the cross-linkage of monoacylated PrP^C does not sequester cholesterol (Fig. 10C), and cross-linkage of desialylated PrP^C does not provide the density of sialic acids that are required to activate cPLA₂ (Fig. 10D). The key role of cPLA₂ in neurodegeneration was supported by our observation that pharmacological inhibition of cPLA₂ reduced the ability of cross-linked PrP^C to trigger synapse degeneration.

In summary, we show that the PrP^{Sc}-induced synapse degeneration was dependent upon the composition of its GPI anchors and could be mimicked by cross-linked PrP^C. The clustering of GPI anchors containing sialic acid activates cPLA₂ and triggers synapse damage. Such observations provide insight into the complex signaling processes that result in prion-induced synapse damage. Moreover, they demonstrate that novel therapies designed to modify GPI anchors may be useful in the treatment of prion diseases.

REFERENCES

1. Stahl, N., Baldwin, M. A., Hecker, R., Pan, K. M., Burlingame, A. L., and Prusiner, S. B. (1992) Glycosylphosphatidylinositol anchors of the scrapie and cellular prion proteins contain sialic acid. *Biochemistry* **31**, 5043–5053
2. Herms, J., Tings, T., Gall, S., Madlung, A., Giese, A., Siebert, H., Schürmann, P., Windl, O., Brose, N., and Kretzschmar, H. (1999) Evidence of presynaptic location and function of the prion protein. *J. Neurosci.* **19**, 8866–8875
3. Salès, N., Rodolfo, K., Hässig, R., Faucheux, B., Di Giamberardino, L., and Moya, K. L. (1998) Cellular prion protein localization in rodent and primate brain. *Eur. J. Neurosci.* **10**, 2464–2471
4. Brown, D. R. (2001) Prion and prejudice: normal protein and the synapse. *Trends Neurosci.* **24**, 85–90
5. Prusiner, S. B. (1998) Prions. *Proc. Natl. Acad. Sci. U.S.A.* **95**, 13363–13383
6. Prusiner, S. B., McKinley, M. P., Bowman, K. A., Bolton, D. C., Bendheim, P. E., Groth, D. F., and Glenner, G. G. (1983) Scrapie prions aggregate to form amyloid-like birefringent rods. *Cell* **35**, 349–358
7. Mayor, S., and Riezman, H. (2004) Sorting GPI-anchored proteins. *Nat. Rev. Mol. Cell Biol.* **5**, 110–120
8. Kimberley, F. C., Sivasankar, B., and Paul Morgan, B. (2007) Alternative roles for CD59. *Mol. Immunol.* **44**, 73–81
9. Rege, T. A., and Hagood, J. S. (2006) Thy-1 as a regulator of cell-cell and cell-matrix interactions in axon regeneration, apoptosis, adhesion, migration, cancer, and fibrosis. *FASEB J.* **20**, 1045–1054
10. Lund-Johansen, F., Olweus, J., Symington, F. W., Arli, A., Thompson, J. S., Vilella, R., Skubitz, K., and Horejsi, V. (1993) Activation of human monocytes and granulocytes by monoclonal antibodies to glycosylphosphatidylinositol-anchored antigens. *Eur. J. Immunol.* **23**, 2782–2791
11. Field, K. A., Holowka, D., and Baird, B. (1995) Fcε RI-mediated recruitment of p53/56lyn to detergent-resistant membrane domains accompanies cellular signaling. *Proc. Natl. Acad. Sci. U.S.A.* **92**, 9201–9205
12. Ikezawa, H. (2002) Glycosylphosphatidylinositol (GPI)-anchored proteins. *Biol. Pharm. Bull.* **25**, 409–417
13. Sun, G. Y., Xu, J., Jensen, M. D., and Simonyi, A. (2004) Phospholipase A₂ in the central nervous system: implications for neurodegenerative diseases. *J. Lipid Res.* **45**, 205–213
14. Horejsi, V., Drbal, K., Cebecauer, M., Cerný, J., Brdicka, T., Angelisová, P., and Stockinger, H. (1999) GPI-microdomains: a role in signaling via immunoreceptors. *Immunol. Today* **20**, 356–361
15. Taraboulos, A., Scott, M., Semenov, A., Avrahami, D., Laszlo, L., Prusiner, S. B., and Avraham, D. (1995) Cholesterol depletion and modification of COOH-terminal targeting sequence of the prion protein inhibit formation of the scrapie isoform. *J. Cell Biol.* **129**, 121–132
16. Kaneko, K., Vey, M., Scott, M., Pilkuhn, S., Cohen, F. E., and Prusiner, S. B. (1997) COOH-terminal sequence of the cellular prion protein directs subcellular trafficking and controls conversion into the scrapie isoform. *Proc. Natl. Acad. Sci. U.S.A.* **94**, 2333–2338
17. Chesebro, B., Trifilo, M., Race, R., Meade-White, K., Teng, C., LaCasse, R., Raymond, L., Favara, C., Baron, G., Priola, S., Caughey, B., Masliah, E., and Oldstone, M. (2005) Anchorless prion protein results in infectious amyloid disease without clinical scrapie. *Science* **308**, 1435–1439
18. Caughey, B., Neary, K., Buller, R., Ernst, D., Perry, L. L., Chesebro, B., and Race, R. E. (1990) Normal and scrapie-associated forms of prion protein differ in their sensitivities to phospholipase and proteases in intact neuroblastoma cells. *J. Virol.* **64**, 1093–1101
19. Atarashi, R., Wilham, J. M., Christensen, L., Hughson, A. G., Moore, R. A., Johnson, L. M., Onwubiko, H. A., Priola, S. A., and Caughey, B. (2008) Simplified ultrasensitive prion detection by recombinant PrP conversion with shaking. *Nat. Methods* **5**, 211–212
20. Bate, C., Tayebi, M., and Williams, A. (2010) The glycosylphosphatidylinositol anchor is a major determinant of prion binding and replication. *Biochem. J.* **428**, 95–101
21. Bate, C., Tayebi, M., and Williams, A. (2010) Phospholipase A₂ inhibitors protect against prion- and Aβ-mediated synapse degeneration. *Mol. Neurodegener.* **5**, 13
22. Cunningham, C., Deacon, R., Wells, H., Boche, D., Waters, S., Diniz, C. P., Scott, H., Rawlins, J. N., and Perry, V. H. (2003) Synaptic changes characterize early behavioral signs in the ME7 model of murine prion disease. *Eur. J. Neurosci.* **17**, 2147–2155
23. Jeffrey, M., Halliday, W. G., Bell, J., Johnston, A. R., MacLeod, N. K., Ingham, C., Sayers, A. R., Brown, D. A., and Fraser, J. R. (2000) Synapse loss associated with abnormal PrP precedes neuronal degeneration in the scrapie-infected murine hippocampus. *Neuropathol. Appl. Neurobiol.* **26**, 41–54
24. Sharma, P., Varma, R., Sarasij, R. C., Ira, Gousset, K., Krishnamoorthy, G., Rao, M., and Mayor, S. (2004) Nanoscale organization of multiple GPI-anchored proteins in living cell membranes. *Cell* **116**, 577–589
25. Suzuki, K. G., Fujiwara, T. K., Sanematsu, F., Iino, R., Edidin, M., and Kusumi, A. (2007) GPI-anchored receptor clusters transiently recruit Lyn and Gα for temporary cluster immobilization and Lyn activation: single-molecule tracking study 1. *J. Cell Biol.* **177**, 717–730
26. McConville, M. J., and Ferguson, M. A. (1993) The structure, biosynthesis and function of glycosylated phosphatidylinositols in the parasitic protozoa and higher eukaryotes. *Biochem. J.* **294**, 305–324
27. Pan, K. M., Stahl, N., and Prusiner, S. B. (1992) Purification and properties of the cellular prion protein from Syrian hamster brain. *Protein Sci.* **1**, 1343–1352
28. Kempster, S., Bate, C., and Williams, A. (2007) Simvastatin treatment prolongs the survival of scrapie-infected mice. *Neuroreport* **18**, 479–482
29. Mok, S. W., Thelen, K. M., Riemer, C., Bamme, T., Gültner, S., Lütjohann, D., and Baier, M. (2006) Simvastatin prolongs survival times in prion infections of the central nervous system. *Biochem. Biophys. Res. Comm.* **348**, 697–702
30. Haviv, Y., Avrahami, D., Ovadia, H., Ben-Hur, T., Gabizon, R., and Sharon, R. (2008) Induced neuroprotection independently from PrP^{Sc} accumulation in a mouse model for prion disease treated with simvastatin. *Arch. Neurol.* **65**, 762–775
31. Mauch, D. H., Nägler, K., Schumacher, S., Göritz, C., Müller, E. C., Otto, A., and Pfrieger, F. W. (2001) CNS synaptogenesis promoted by glia-derived cholesterol. *Science* **294**, 1354–1357
32. Farooqui, A. A., Horrocks, L. A., and Farooqui, T. (2007) Modulation of inflammation in brain: a matter of fat. *J. Neurochem.* **101**, 577–599
33. Malaplate-Armand, C., Florent-Béchar, S., Youssef, I., Koziel, V.,

- Sponne, I., Kriem, B., Leininger-Muller, B., Olivier, J. L., Oster, T., and Pillot, T. (2006) Soluble oligomers of amyloid- β peptide induce neuronal apoptosis by activating a cPLA₂-dependent sphingomyelinase-ceramide pathway. *Neurobiol. Dis.* **23**, 178–189
34. Sanchez-Mejia, R. O., Newman, J. W., Toh, S., Yu, G. Q., Zhou, Y., Halabisky, B., Cissé, M., Searce-Levie, K., Cheng, I. H., Gan, L., Palop, J. J., Bonventre, J. V., and Mucke, L. (2008) Phospholipase A₂ reduction ameliorates cognitive deficits in a mouse model of Alzheimer disease. *Nat. Neurosci.* **11**, 1311–1318
35. Stuermer, C. A., Langhorst, M. F., Wiechers, M. F., Legler, D. F., Von Hanwehr, S. H., Guse, A. H., and Plattner, H. (2004) PrP^{Sc} capping in T cells promotes its association with the lipid raft proteins reggie-1 and reggie-2 and leads to signal transduction. *FASEB J.* **18**, 1731–1733
36. Solforsio, L., Criado, J. R., McGavern, D. B., Wirz, S., Sánchez-Alavez, M., Sugama, S., DeGiorgio, L. A., Volpe, B. T., Wiseman, E., Abalos, G., Masliah, E., Gilden, D., Oldstone, M. B., Conti, B., and Williamson, R. A. (2004) Cross-linking cellular prion protein triggers neuronal apoptosis *in vivo*. *Science* **303**, 1514–1516
37. Chiesa, R., Piccardo, P., Biasini, E., Ghetti, B., and Harris, D. A. (2008) Aggregated, wild-type prion protein causes neurological dysfunction and synaptic abnormalities. *J. Neurosci.* **28**, 13258–13267
38. Homans, S. W., Ferguson, M. A., Dwek, R. A., Rademacher, T. W., Anand, R., and Williams, A. F. (1988) Complete structure of the glycosyl phosphatidylinositol membrane anchor of rat brain Thy-1 glycoprotein. *Nature* **333**, 269–272
39. Cenedella, R. J. (2009) Cholesterol synthesis inhibitor U18666A and the role of sterol metabolism and trafficking in numerous pathophysiological processes. *Lipids* **44**, 477–487
40. Puglielli, L., Tanzi, R. E., and Kovacs, D. M. (2003) Alzheimer disease: the cholesterol connection. *Nat. Neurosci.* **6**, 345–351
41. Stefani, M., and Liguri, G. (2009) Cholesterol in Alzheimer disease: unresolved questions. *Curr. Alzheimer Res.* **6**, 15–29
42. Vey, M., Pilkuhn, S., Wille, H., Nixon, R., DeArmond, S. J., Smart, E. J., Anderson, R. G., Taraboulos, A., and Prusiner, S. B. (1996) Subcellular colocalization of the cellular and scrapie prion proteins in caveolae-like membranous domains. *Proc. Natl. Acad. Sci. U. S. A.* **93**, 14945–14949
43. Naslavsky, N., Stein, R., Yanai, A., Friedlander, G., and Taraboulos, A. (1997) Characterization of detergent-insoluble complexes containing the cellular prion protein and its scrapie isoform. *J. Biol. Chem.* **272**, 6324–6331
44. Schroeder, R., London, E., and Brown, D. (1994) Interactions between saturated acyl chains confer detergent resistance on lipids and glycosylphosphatidylinositol (GPI)-anchored proteins: GPI-anchored proteins in liposomes and cells show similar behavior. *Proc. Natl. Acad. Sci. U. S. A.* **91**, 12130–12134
45. Anderson, R. G., and Jacobson, K. (2002) A role for lipid shells in targeting proteins to caveolae, rafts, and other lipid domains. *Science* **296**, 1821–1825
46. Brügger, B., Graham, C., Leibrecht, I., Mombelli, E., Jen, A., Wieland, F., and Morris, R. (2004) The membrane domains occupied by glycosylphosphatidylinositol-anchored prion protein and Thy-1 differ in lipid composition. *J. Biol. Chem.* **279**, 7530–7536
47. Pike, L. J. (2004) Lipid rafts: heterogeneity on the high seas. *Biochem. J.* **378**, 281–292
48. Simons, K., and Ikonen, E. (1997) Functional rafts in cell membranes. *Nature* **387**, 569–572
49. Eisenberg, S., Shvartsman, D. E., Ehrlich, M., and Henis, Y. I. (2006) Clustering of raft-associated proteins in the external membrane leaflet modulates internal leaflet H-ras diffusion and signaling. *Mol. Cell. Biol.* **26**, 7190–7200
50. Gri, G., Molon, B., Manes, S., Pozzan, T., and Viola, A. (2004) The inner side of T cell lipid rafts. *Immunol. Lett.* **94**, 247–252
51. Montixi, C., Langlet, C., Bernard, A. M., Thimonier, J., Dubois, C., Wurzel, M. A., Chauvin, J. P., Pierres, M., and He, H. T. (1998) Engagement of T cell receptor triggers its recruitment to low-density detergent-insoluble membrane domains. *EMBO J.* **17**, 5334–5348
52. Mouillet-Richard, S., Ermonval, M., Chebassier, C., Laplanche, J. L., Lehmann, S., Launay, J. M., and Kellermann, O. (2000) Signal transduction through prion protein. *Science* **289**, 1925–1928
53. Chiarini, L. B., Freitas, A. R., Zanata, S. M., Brentani, R. R., Martins, V. R., and Linden, R. (2002) Cellular prion protein transduces neuroprotective signals. *EMBO J.* **21**, 3317–3326